Report

Cell Reports

The Microtubule Minus-End-Binding Protein Patronin/PTRN-1 Is Required for Axon Regeneration in *C. elegans*

Graphical Abstract

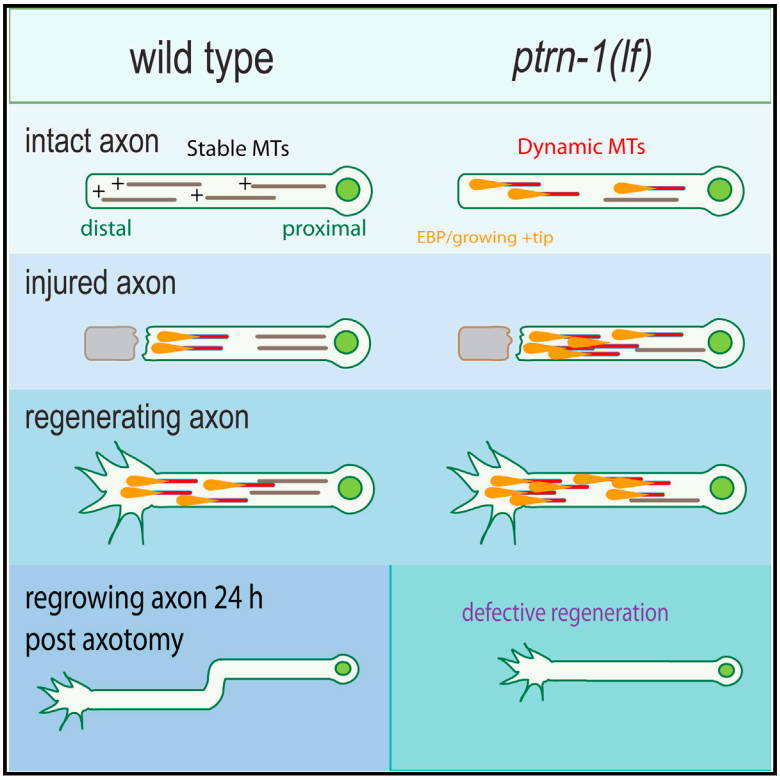

Highlights

Axon regeneration is defective in *C. elegans ptrn-1* (Patronin/CAMSAP) mutants

PTRN-1 restrains microtubule dynamics in the mature and regrowing axon

The PTRN-1 CKK domain is necessary and sufficient for its function in axon regrowth

PTRN-1 and DLK-1 are both required for normal axon regrowth.

Authors

Marian Chuang, Alexandr Goncharov, ..., Yishi Jin, Andrew D. Chisholm

Correspondence

chisholm@ucsd.edu

In Brief

Proper axon regeneration requires precise regulation of microtubule (MT) dynamics. Chuang et al. show that *C. elegans* mutants lacking PTRN-1, the ortholog of the Patronin/CAMSAP MT minus-end-binding proteins, display inefficient axon regeneration. *ptrn-1* mutants display increased axonal MT dynamics, and suppression of these dynamics is correlated with rescued axon regrowth. PTRN-1 may function in axon regeneration by stabilizing MTs.

Chuang et al., 2014, Cell Reports 9, 874–883
November 6, 2014 ©2014 The Authors
http://dx.doi.org/10.1016/j.celrep.2014.09.054

OPEN ACCESS
CellPress

Cell Reports
Report

The Microtubule Minus-End-Binding Protein Patronin/PTRN-1 Is Required for Axon Regeneration in *C. elegans*

Marian Chuang,[1] Alexandr Goncharov,[2] Shaohe Wang,[3,4,5] Karen Oegema,[3,4] Yishi Jin,[1,2,3] and Andrew D. Chisholm[1,*]
[1]Section of Neurobiology, Division of Biological Sciences, University of California, San Diego, La Jolla, CA 92093, USA
[2]Howard Hughes Medical Institute
[3]Department of Cellular and Molecular Medicine
University of California, San Diego, La Jolla, CA 92093, USA
[4]Ludwig Institute for Cancer Research
[5]Biomedical Sciences Graduate Program
University of California, San Diego, La Jolla, CA 92093, USA
*Correspondence: chisholm@ucsd.edu
http://dx.doi.org/10.1016/j.celrep.2014.09.054

SUMMARY

Precise regulation of microtubule (MT) dynamics is increasingly recognized as a critical determinant of axon regeneration. In contrast to developing neurons, mature axons exhibit noncentrosomal microtubule nucleation. The factors regulating noncentrosomal MT architecture in axon regeneration remain poorly understood. We report that PTRN-1, the *C. elegans* member of the Patronin/Nezha/calmodulin- and spectrin-associated protein (CAMSAP) family of microtubule minus-end-binding proteins, is critical for efficient axon regeneration in vivo. *ptrn-1*-null mutants display generally normal developmental axon outgrowth but significantly impaired regenerative regrowth after laser axotomy. Unexpectedly, mature axons in *ptrn-1* mutants display elevated numbers of dynamic axonal MTs before and after injury, suggesting that PTRN-1 inhibits MT dynamics. The CKK domain of PTRN-1 is necessary and sufficient for its functions in axon regeneration and MT dynamics and appears to stabilize MTs independent of minus-end localization. Whereas in developing neurons, PTRN-1 inhibits activity of the DLK-1 mitogen-activated protein kinase (MAPK) cascade, we find that, in regeneration, PTRN-1 and DLK-1 function together to promote axonal regrowth.

INTRODUCTION

The ability of axons to regenerate their structure after injury is now recognized as a fundamental and conserved property of neurons. The ability of axons to regrow in vivo is modulated by a large number of interacting influences, including the extracellular microenvironment and the intrinsic growth state of the neuron. Recent studies have begun to reveal the molecular determinants of the neuronal growth state (Liu et al., 2011). In vertebrate neurons, intrinsic determinants of axon regrowth include PTEN (Park et al., 2008) and the KLF transcription factors (Moore et al., 2009). Studies of axon regrowth in genetic model organisms such as *C. elegans* have also contributed to our understanding of axon regeneration mechanisms (Hammarlund and Jin, 2014). In *C. elegans*, the DLK-1 mitogen-activated protein kinase cascade has been revealed as a key intrinsic regulator of regrowth initiation and may act to sense axonal damage (Hammarlund et al., 2009; Yan and Jin, 2012; Yan et al., 2009). DLK kinases also play critical roles in axon regrowth in *Drosophila* and mammals (Tedeschi and Bradke, 2013; Xiong et al., 2010).

Regulation of axonal microtubule (MT) dynamics has emerged as a key factor in axonal regrowth potential. The MT network of mature axons is largely composed of stable MTs. Axon injury triggers an intricate series of changes in axonal MT organization and dynamics that drive formation of regenerative growth cones and subsequent axon extension (Bradke et al., 2012; Chisholm, 2013). After injury, microtubule dynamics are upregulated by a variety of mechanisms (Sahly et al., 2006; Stone et al., 2010). Interestingly, partial stabilization of axonal MTs by pharmacological treatment after spinal cord injury promotes axon regrowth (Hellal et al., 2011; Sengottuvel et al., 2011). Loss of function in MT destabilization factors can enhance axon regrowth in *C. elegans* (Chen et al., 2011; Ghosh-Roy et al., 2012). Conversely, failure to regenerate correlates with disorganization of the axonal MT cytoskeleton (Ertürk et al., 2007). These studies highlight the importance of MT remodeling as a conserved intrinsic determinant of axon regeneration capacity.

In dividing cells, the centrosome is the dominant microtubule-organizing center. In contrast, the MT cytoskeleton of neurons is predominantly noncentrosomal (Keating and Borisy, 1999). A well-established model for axonal MT biogenesis is that axonal MTs are nucleated at the centrosome and then cleaved and translocated into the axon during axonal development and regeneration (Conde and Cáceres, 2009). At least some axonal MTs can form independently of the centrosome in mammalian neurons (Stiess et al., 2010). In *Drosophila* neurons, MT organization is unaltered by laser ablation or mutational disruption of

the centrosome (Nguyen et al., 2011); γ-tubulin at noncentrosomal sites is required for MT nucleation (Nguyen et al., 2014; Ori-McKenney et al., 2012). The control of noncentrosomal MT stabilization in neuronal processes remains poorly understood.

The Patronin/Nezha/calmodulin- and spectrin-associated protein (CAMSAP) MT-binding proteins regulate noncentrosomal MT architecture in a variety of cell types. CAMSAPs can bind specifically (Meng et al., 2008) and directly to MT minus ends (Goodwin and Vale, 2010; Hendershott and Vale, 2014; Jiang et al., 2014). Of the three mammalian CAMSAPs, CAMSAP2 is important for axon specification and dendrite morphology in mouse hippocampal neurons (Yau et al., 2014). *C. elegans* encodes a single Patronin/CAMSAP, PTRN-1. *ptrn-1*-null mutants are viable and superficially normal in behavior and morphology but are hypersensitive to MT-destabilizing drugs (Marcette et al., 2014; Richardson et al., 2014). Neurons of *ptrn-1*-null mutants display impenetrant axon overgrowth defects that may result from activation of a regenerative program involving the DLK-1 cascade. However, the role of Patronins in axon regeneration has not been directly evaluated.

Here, we report that *ptrn-1* mutants are impaired in axon regeneration, in contrast to their near-normal developmental axon outgrowth. The requirement for PTRN-1 in regeneration is bypassed by loss of function in the MT depolymerase kinesin-13/KLP-7. *ptrn-1* mutants display reduced numbers of axonal MTs yet have increased numbers of dynamic axonal MTs. The aberrant MT dynamics of *ptrn-1* mutants are suppressed by loss of function in the DLK-1 pathway. Despite this, PTRN-1 can act independently of DLK-1 in regeneration and PTRN-1 overexpression induces branches in *dlk-1*-null mutants. We conclude that PTRN-1 plays a critical role in noncentrosomal MT dynamics in axon regrowth and that the relationship of PTRN-1 and DLK-1 in regeneration is distinct from that in development.

RESULTS

C. elegans Patronin/PTRN-1 Is Required for Axon Regeneration

To address the role of PTRN-1 in axon regeneration, we examined three *ptrn-1* putative null mutant alleles, collectively, *ptrn-1*(*0*) (see Experimental Procedures). We confirmed previous findings that *ptrn-1*(*0*) mutants are viable and superficially normal in behavior, with incompletely penetrant defects in touch neuron morphology (Marcette et al., 2014). For example, in *ptrn-1*(*0*) mutants, the cell bodies of ALM neurons extend ectopic posterior neurites of varying lengths (Figure S1A). Nonetheless, PTRN-1 is generally dispensable for developmental axon outgrowth.

To investigate roles of PTRN-1 in axon regeneration, we used femtosecond laser surgery to sever the PLM axon in *ptrn-1*(*0*) mutants and imaged axon regrowth. PLM axon regrowth was significantly impaired in *ptrn-1*(*0*) mutants, decreasing to 60%–75% of wild-type regrowth at 24 hr postaxotomy (24 hpa) (Figures 1A and 1B). The PLM regeneration defects of *ptrn-1*(*0*) mutants were rescued by panneural expression of PTRN-1, consistent with PTRN-1 acting cell autonomously (Figures 1A and 1B). Panneural overexpression of PTRN-1 in wild-type background did not enhance PLM regrowth (Figure 1A), suggesting PTRN-1 levels are not rate limiting in regeneration. In *ptrn-1*(*lt1*) and *ptrn-1*(*tm5597*) mutants, and to a lesser extent in *ptrn-1*(*ju698*), axotomy of PLM occasionally triggered growth of small neurites ("sprouting") from the soma (Figures 1B and S1B); this phenotype was rescued by PTRN-1::GFP transgenes (Figure S1B). Regeneration of commissures of D-type motor neurons was also impaired in *ptrn-1* mutants (Figures S1C and S1D), indicating PTRN-1 is required for regeneration of diverse neuron types.

Reduced axon regrowth may reflect defects in axon extension or in growth cone formation (Chen et al., 2011). We examined PLM regrowth in *ptrn-1*(*0*) at 6 and 48 hpa and found that regrowth was significantly reduced at all time points (Figure 1C), reflecting a reduced rate of PLM axon extension throughout the period of regrowth (Figure 1D). *ptrn-1*(*0*) mutant axons formed regenerative growth cones at similar frequencies to the wild-type at 6 and 24 hpa; by 48 hpa, growth cones remained in *ptrn-1*(*0*) mutants but were mostly absent from wild-type axons (Figure 1E). Thus, PTRN-1 is not required for formation of regenerative growth cones; the persistence of growth cones at 48 hpa may reflect slower regrowth of *ptrn-1* axons.

To define when in regrowth PTRN-1 was required, we induced PTRN-1 expression at different times relative to axotomy and assayed rescue of the *ptrn-1*(*0*) regrowth phenotypes at 24 hpa (see Experimental Procedures). Induction of PTRN-1 4 hr or 1 hr before axotomy fully rescued *ptrn-1*(*0*) regrowth defects (Figure 1F). In contrast, induction at 6 hpa failed to rescue *ptrn-1*(*0*) (Figure 1F), suggesting PTRN-1 function is required within the first 6 hr after injury and that the decreased regrowth of *ptrn-1*(*0*) is not caused by earlier developmental defects.

We further probed the temporal requirements for PTRN-1 function by protein inhibition using miniSOG-based chromophore-assisted light inactivation (CALI). miniSOG absorbs blue light and generates singlet oxygen when illuminated with high-intensity blue light (Shu et al., 2011), allowing inactivation of tagged proteins via CALI (Lin et al., 2013; Zhou et al., 2013). PTRN-1::miniSOG rescued the regrowth defects of *ptrn-1*(*0*) neurons (Figure 1G). Illumination with blue light a few minutes before axotomy abolished *ptrn-1* rescuing activity (Figure 1G), suggesting PTRN-1::miniSOG was efficiently inactivated by CALI. Panneuronal expression of a control construct expressing cytosolic miniSOG did not affect regrowth, with or without blue light treatment. We then used blue light illumination at different times to dissect when PTRN-1 was required. Illumination 6 hr before, or minutes prior to axotomy ("0 hr"), abolished PTRN-1::miniSOG rescuing activity, whereas inactivation 6 hpa only partly inhibited PTRN-1 function (Figure 1G), consistent with PTRN-1 being required in the first few hours after axon injury.

Axonal MT Dynamics Are Upregulated in *ptrn-1*(*0*) mutants before and after Axon Injury

ptrn-1(*0*) mutants display fewer dynamic MTs in PHC dendrites and are sensitized to MT-depolymerizing drugs, suggesting PTRN-1 stabilizes MTs (Richardson et al., 2014). We therefore tested whether the impaired axon regeneration of *ptrn-1*(*0*) mutants reflected altered MT dynamics, using GFP-tagged end-binding protein (EBP) to track growing MT plus ends

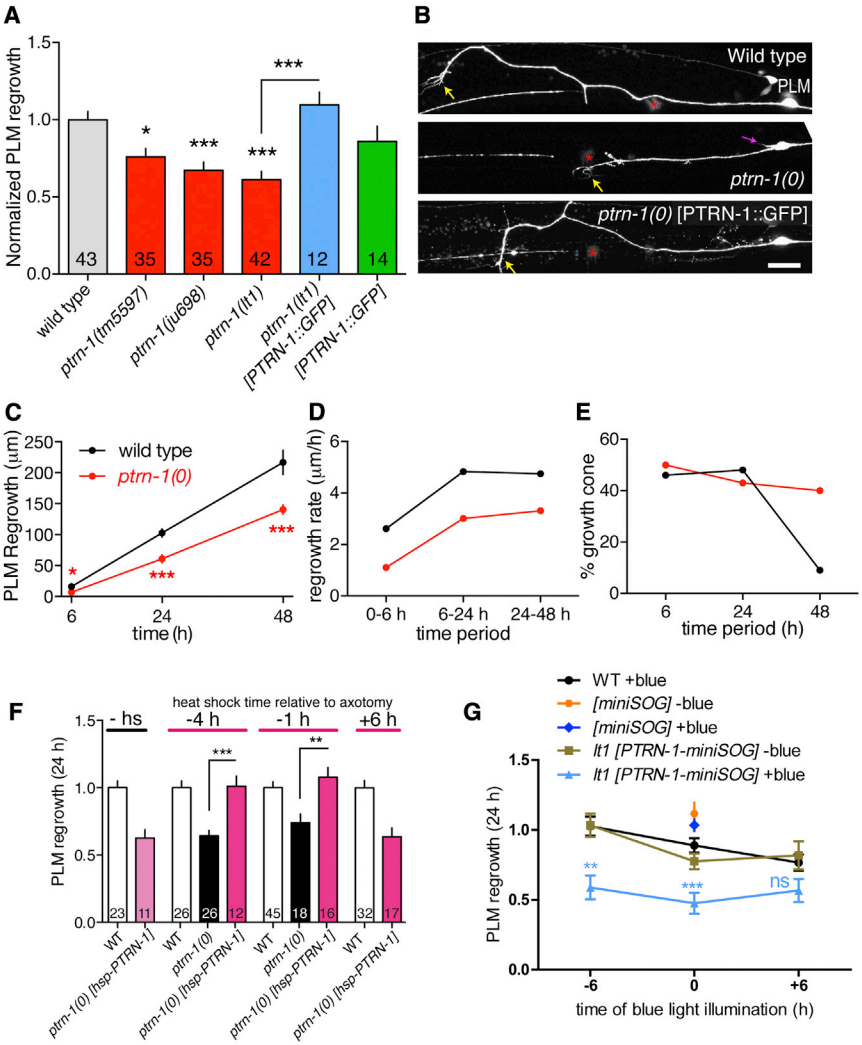

Figure 1. PTRN-1 Is Required for Sensory and Motor Neuron Axon Regeneration

(A) PLM axon regrowth is significantly reduced in *ptrn-1*(*0*) mutants and fully rescued by panneural expression of PTRN-1 (P*rgef-1*-PTRN-1::GFP, *juEx5676*). Bars indicate mean ± SEM. Statistics: Kruskal-Wallis test and Dunn's posttest; *p < 0.05; ***p < 0.001.

(B) PLM axons (*muIs32*) at 24 hpa in wild-type, *ptrn-1*(*lt1*), and *ptrn-1*(*lt1*) rescued by P*rgef-1*-PTRN-1::GFP(*juEx5676*). Anterior is to the left and dorsal up; red asterisks, site of axotomy. Regenerative growth cones (yellow arrows) are normal in *ptrn-1*(*0*) mutants. Axon injury in *ptrn-1*(*lt1*) triggers sprouting of extra neurites from the PLM soma in ~20% of animals (magenta arrow; Figure S1B).

(C) *ptrn-1*(*lt1*) mutants display reduced regrowth throughout PLM regeneration.

(D) *ptrn-1*(*lt1*) mutants display reduced axon extension rates.

(E) In *ptrn-1*(*lt1*) mutants, regrowing axons retain growth cones at 48 hpa.

(F) The *ptrn-1*(*lt1*) regrowth defect is rescued by heat-shock-induced expression of PTRN-1 either 4 hr or 1 hr before axotomy, but not by heat shock at 6 hpa. Animals were heat shocked at 34°C for 1 hr. Bars indicate mean ± SEM. Statistics: Student's t test; ***p < 0.001; **p < 0.01.

(G) PTRN-1::miniSOG-induced CALI at 6 hr or 0 hr prior to axotomy abolishes PTRN-1 rescue activity, whereas CALI at +6 hr does not significantly reduce rescue. Bars indicate mean ± SEM.

(H) PLM regrowth is normalized to WT of corresponding time point in the absence of blue light. Genotypes: wild-type (*muIs32*), panneural cytosolic miniSOG (*juEx3701*), and *ptrn-1*(*lt1*); P*rgef-1*-PTRN-1::miniSOG (*juEx6307*). Kruskal-Wallis test, Dunn posttest; ***p < 0.001 compared to WT + blue light at same time point.

(Ghosh-Roy et al., 2012; Stepanova et al., 2003). In the wild-type, uninjured PLM axon, few EBP comets are visible, consistent with most MTs being stabilized (Ghosh-Roy et al., 2012). In contrast, *ptrn-1*(*0*) mutants displayed a 2-fold increase in the number of axonal EBP comets in the steady state, as well as increased comet growth velocity and persistence (Figures 2A–2C and S2A). Altered MT dynamics in *ptrn-1*(*0*) mutants were rescued by panneuronally expressed PTRN-1 (Figures 2A–2C). Overexpression of PTRN-1 in wild-type backgrounds did not significantly alter MT dynamics (Figures 2A–2C), consistent with its lack of effect on axon regeneration. Axonal MT polarity was normal in *ptrn-1*(*0*) or in *ptrn-1*(++) backgrounds (Figure S3). We conclude that PTRN-1 specifically restrains the number of dynamic MTs in axons.

C. elegans touch neurons contain many 15-protofilament (pf) MTs, as opposed to the 11 pf MTs prevalent in other *C. elegans* neurons or the 13 pf MTs typical of neurons in other species (Topalidou et al., 2012). To assess whether PTRN-1 repressed dynamic MTs in other neurons, we examined D-type motor neurons, which contain a small number of 11 pf MTs. As in PLM, *ptrn-1*(*0*) D neurons displayed increased numbers of dynamic MTs (Figures S2B and S2C). Thus, *ptrn-1* mutants display more dynamic MTs in axons with different MT types.

Axotomy of PLM axons results in an increase in the number of dynamic MTs by 3 hr after injury followed by a decrease in catastrophe frequency concurrent with growth cone formation (Ghosh-Roy et al., 2012; Figures 2E–2G). In *ptrn-1*(*0*) mutants, the numbers and growth length of dynamic MTs 3 hpa were further elevated compared to wild-type (Figure 3E). Thus, despite displaying more dynamic MTs in the steady state, *ptrn-1*(*0*) mutants can respond to injury by further increasing dynamic MT numbers.

Axonal MTs in *ptrn-1*(*0*) Mutants Are Reduced in Number and Increased in Length but Display Normal Minus-End Morphology

The increased MT growth velocity in uninjured axons of *ptrn-1*(*0*) might be explained by elevated tubulin concentration due to reduced total MT polymers. Ultrastructural analysis of *ptrn-1*(*tm5597*) mutants showed that PLM axons contained fewer MTs than in the wild-type (Richardson et al., 2014). Here, we performed serial section electron microscopy on *ptrn-1*(*lt1*)

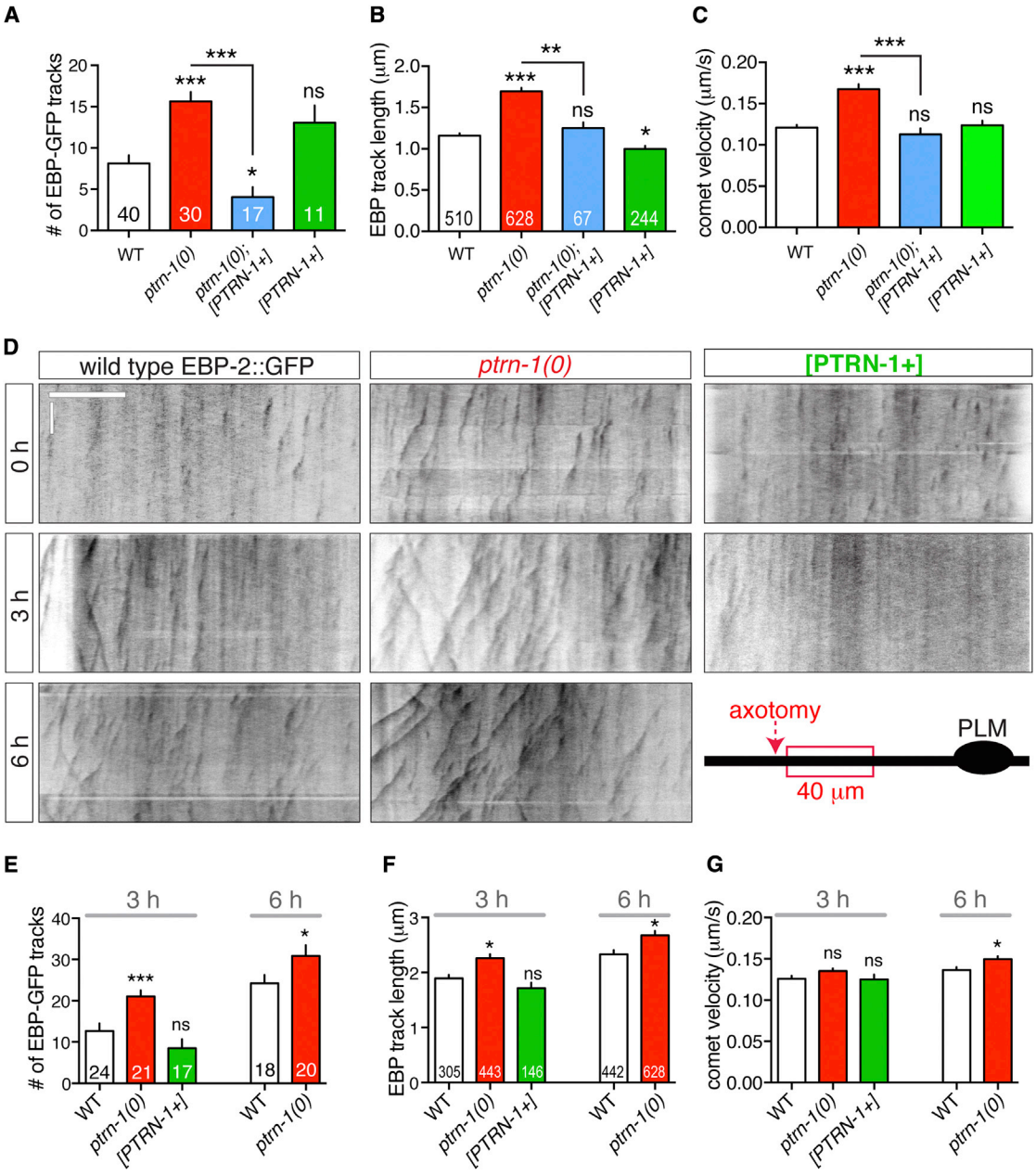

Figure 2. *ptrn-1* Mutants Display Elevated Numbers of Dynamic Axonal Microtubules before and after Axon Injury

(A–C) Quantitation of MT plus-end dynamics in the uninjured PLM axon using P*mec-4*-EBP-2::GFP(*juIs338*). Bars show mean ± SEM; statistics: ANOVA and Sidak posttest. (A) *ptrn-1*(*lt1*) mutants display more EBP-2::GFP comets in the PLM axon prior to axotomy; this phenotype is rescued by panneural expression of PTRN-1(*juEx5580*); overexpression of PTRN-1 in wild-type background does not significantly affect MT dynamics. In (A) and (E), numbers on bars indicate number of axons. (B) EBP-2::GFP track length is significantly increased in *ptrn-1*(*lt1*) mutants. Statistics (B and C): Kruskal-Wallis test and Dunn's posttest. In (B) and (F), numbers on bars indicate number of tracks; same tracks analyzed in (C) and (G). (C) EBP-2::GFP comets grow faster in *ptrn-1*(*lt1*) PLM axons.

(D) Representative kymographs (inverted grayscale) of EBP-2::GFP (*juIs338*) tracks in WT and *ptrn-1*(*lt1*) and PTRN[+] (*juEx6178*) PLM axons, before and 3 and 6 hr after axotomy. In all kymographs of PLM, the length (x axis) and time (y axis) scales are 10 μm and 10 s, respectively.

(E–G) *ptrn-1*(*lt1*) mutants have increased numbers of dynamic MTs, EBP track length, and velocity at 3 and 6 hr postinjury compared to wild-type; n > 10 axons per genotype. Statistics: Kruskal-Wallis test (3 hr); Mann-Whitney test (6 hr).

and *ptrn-1*(*ju698*) mutants and counted MTs in ALM and PLM axons (Table S1). In wild-type PLM axons, MT numbers average 46 (four axons) whereas *ptrn-1*(*lt1*) animals had an average of 17 (range 12–24; 40 sections from two axons), revealing a trend of reduced axonal MTs. We did not observe small-diameter or morphologically aberrant MTs as reported

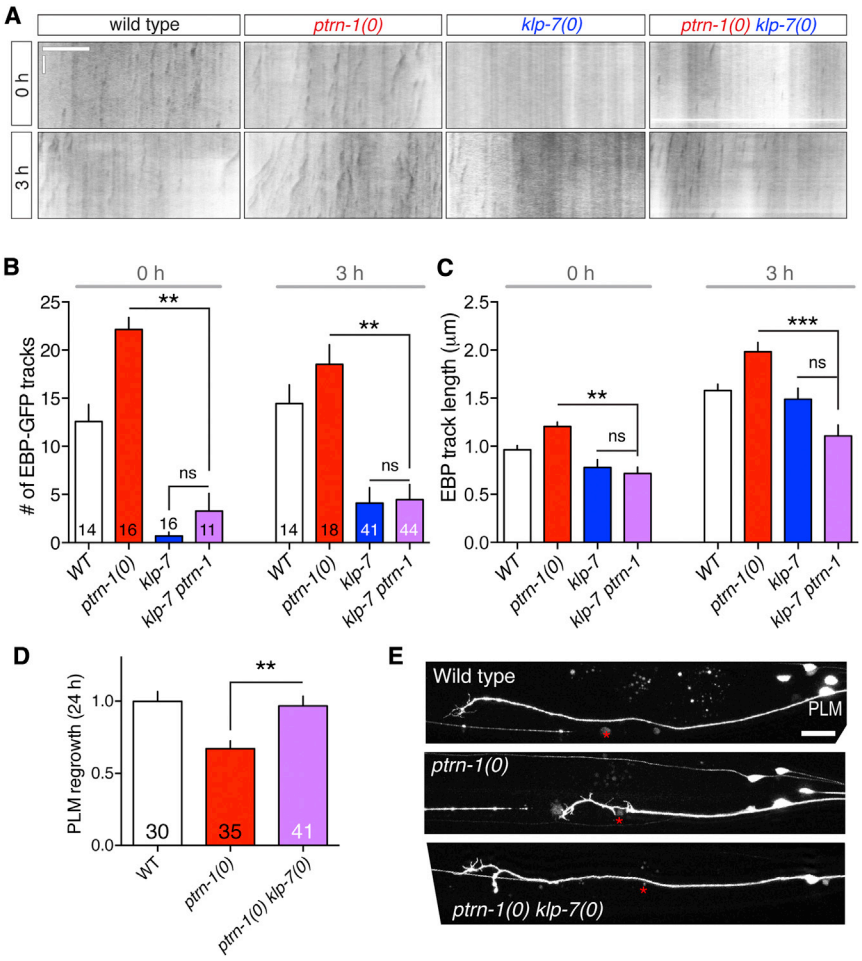

Figure 3. *ptrn-1*(*0*) Defects in MT Dynamics and Axon Regeneration Are Suppressed by Loss of Kinesin-13/KLP-7

(A) Representative kymographs of P*mec-4*-EBP-2::GFP(*juIs338*) dynamics in PLM axons, before and after injury. *klp-7*(*tm2143*) mutants display few dynamic MTs before injury and upregulate MT dynamics at 3 hr postinjury.

(B) Quantitation of EBP::GFP track numbers before and 3 hr after injury; n > 10 axons per condition.

(C) *klp-7*(*tm2143*) suppresses the increased EBP::GFP track length of *ptrn-1*(*lt1*); n > 70 tracks per condition. Bars indicate mean ± SEM. Statistics: Kruskal-Wallis test. ***p < 0.001; **p < 0.01.

(D and E) The *ptrn-1*(*ju698*) defect in PLM axonal regrowth is suppressed by the *klp-7*(*tm2143*)-null mutation; *klp-7* single mutants display normal regrowth (Ghosh-Roy et al., 2012); scale: 10 μm. Statistics: t test.

for *ptrn-1*(*tm5597*) (Richardson et al., 2014); this may reflect the different axonal regions examined or other differences in genetic background.

As PTRN-1 has been implicated in stabilization or anchoring of MT minus ends in neurons, we reconstructed the MT arrays of an ALM axon segment in wild-type and *ptrn-1*(*0*) animals (Figure S4). Counting fully reconstructed MTs, wild-type axons contained 8.9 minus ends/μm, whereas in *ptrn-1*(*ju698*), we saw 1.7 minus ends/μm, a 5-fold reduction in density of minus ends. Interestingly, *ptrn-1*(*ju698*) mutants also displayed significantly longer individual MTs (7.3 ± 0.8 μm versus 3.3 ± 0.2 μm in the wild-type), so the number of MT profiles per section is reduced only 2-fold in *ptrn-1*. We also examined MT end morphology; when an MT end is imaged in a thin section, it appears as diffuse (corresponding to the splayed MT lattice at the plus end) or filled (minus end; Chalfie and Thomson, 1979; Figure S4A). MT terminations not imaged close to the section surface resemble the rest of the MT and are scored as clear. Most fully reconstructed MTs had diffuse plus distal ends both in the wild-type and in *ptrn-1*(*ju698*) mutants (83% in wild-type [WT] versus 79% in mutant). A small fraction of MTs have filled/minus ends distal (24% in WT versus 38% in mutant). This analysis suggests that PTRN-1 does not affect the ultrastructure or orientation of MT ends.

ptrn-1 Defects in MT Dynamics and Axon Regrowth Are Suppressed by Loss of Function in the MT Depolymerizing Kinesin-13/KLP-7

To address mechanistically why PTRN-1 is required for axon regrowth, we investigated its potential interactors. In *Drosophila*, Patronin protects MT minus ends from kinesin-13-mediated depolymerization (Goodwin and Vale, 2010; Wang et al., 2013). In *C. elegans*, KLP-7/kinesin-13 destabilizes axonal MTs (Ghosh-Roy et al., 2012). To address whether reduced axon regeneration of *ptrn-1*(*0*) might reflect excessive KLP-7-dependent depolymerization of MT minus ends, we analyzed MT dynamics in *ptrn-1*(*0*) *klp-7*(*0*) double mutants. Few or no EBP comets were visible in *klp-7*(*0*) axons, and *klp-7*(*0*) *ptrn-1*(*0*) double mutants resembled *klp-7*(*0*) (Figures 3A–3C). The track length of individual EBP comets in *ptrn-1*(*0*) *klp-7*(*0*) double mutants was suppressed to wild-type levels (Figure 3C). *ptrn-1*(*0*) *klp-7*(*0*) double mutants displayed reduced MT dynamics after injury (Figures 3A–3C). These data indicate that the elevated number of growing MTs in *ptrn-1*(*0*) requires KLP-7. Remarkably, PLM regrowth was suppressed to wild-type levels in the *ptrn-1*(*0*) *klp-7*(*0*) double mutant (Figures 3D and 3E). Thus, the requirement for PTRN-1 can be bypassed by loss of KLP-7, suggesting the inability of *ptrn-1*(*0*) axons to regrow is due to KLP-7-mediated MT depolymerization.

The CKK Domain of PTRN-1 Is Necessary and Sufficient for PTRN-1 Function in Axon Regeneration

To elucidate the roles of PTRN-1 domains in axon regeneration, we expressed fragments and domains of PTRN-1 (Figure 4A). PTRN-1, like other CAMSAPs, contains an N-terminal calponin homology (CH) domain, a coiled-coil region, and a C-terminal CAMSAP/KIAA1078/KIAA1543 (CKK) domain. The CKK domain is unique to the CAMSAP family and binds MTs (Baines et al.,

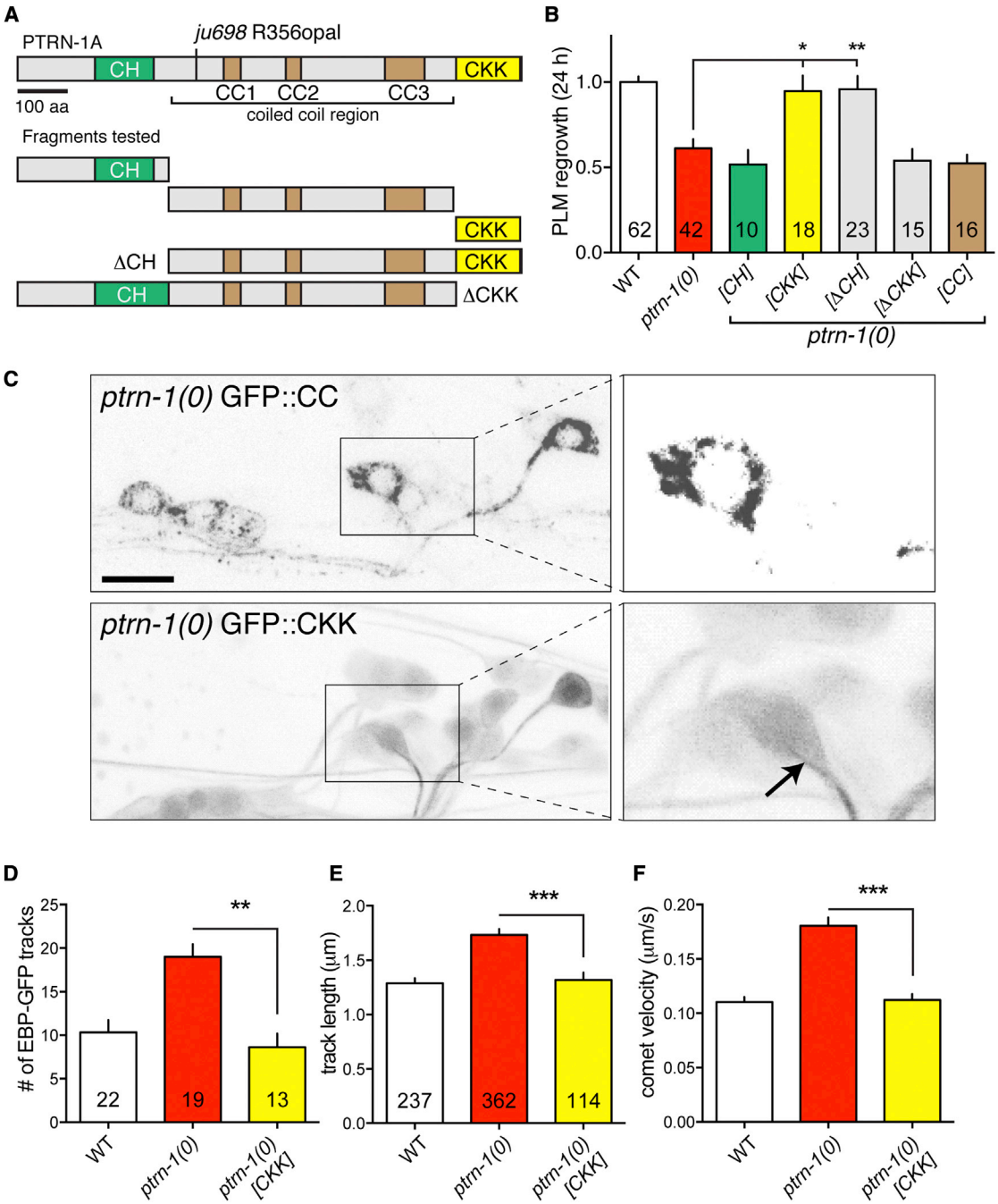

Figure 4. The CKK Domain of PTRN-1 Is Necessary and Sufficient for Its Function in Axon Regeneration and Inhibition of Dynamic MTs

(A) Domain architecture of PTRN-1 full-length and fragments and *ju698* mutation. PTRN-1A contains a calponin homology (CH) domain (amino acid [aas] 153–270), three coiled-coil (CC) regions, and a CKK domain (aas 969–1098).

(B) Expression of the CKK domain is sufficient to rescue *ptrn-1*(*lt1*) axon regrowth defects to wild-type levels. Bars indicate mean ± SEM. Statistics: Kruskal-Wallis test, Dunn posttest; ***p < 0.001; **p < 0.01 compared to *ptrn-1*(*lt1*).

(C) The coiled coil domain (GFP::CC, *juEx6308*) displays similar localization to full-length PTRN-1 (see Figure S5) in a *ptrn-1*(*lt1*) mutant background. In contrast, the GFP::CKK fusion protein (*juEx6311*) is largely diffuse but displays faint filamentous localization in proximal axons (arrow).

(D–F) Expression of the CKK domain alone is sufficient to rescue the increased EBP::GFP (*juIs338*) dynamics of *ptrn-1*(*lt1*) in the uninjured PLM. Bars indicate mean ± SEM. Statistics: Kruskal-Wallis test, Dunn's posttest.

2009; Goodwin and Vale, 2010; Jiang et al., 2014). The domain responsible for minus-end targeting varies: in human CAMSAPs, the CKK domains are sufficient for minus-end targeting (Jiang et al., 2014), whereas in *Drosophila* Patronin, the CKK domain binds along the length of MTs and the coiled-coil region is required for minus-end targeting (Goodwin and Vale, 2010). We found that transgenic overexpression of the CKK domain, but not the CH or the coiled-coil domains, was both necessary and sufficient to rescue regrowth defects of *ptrn-1*(*0*) (Figure 4B). CKK domain overexpression in a *ptrn-1*(*0*) background also caused formation of long ALM posterior neurites (not shown), as seen in other conditions where axonal MTs are hyperstabilized (Ghosh-Roy et al., 2012; Kirszenblat et al., 2013). Consistent with the idea that the CKK domain stabilizes MTs, we found that overexpression of the CKK domain in a *ptrn-1*(*0*) background reduced the number, length, and velocity of EBP tracks (Figures 4D–4F).

To investigate how the PTRN-1 domains might contribute to axonal regrowth, we examined their subcellular localization. PTRN-1 has been shown to localize to puncta along the processes of many neurons (Richardson et al., 2014); we confirmed this with our functional tagged PTRN-1 fusion proteins, expressed either from single-copy insertion transgenes containing the *ptrn-1* promoter or under the control of other neuronal promoters (Figure S5). PTRN-1::GFP puncta were dense in touch neurons (e.g., Figures S5D and S5F), whereas puncta in motor neuron commissures were more sparse (Figures S5D and S5E), correlating with their lower density of axonal MTs. In other neurons, PTRN-1::GFP was predominantly punctate (Figure S5B), although some filaments were seen in axons (Figure S5C). Puncta could also be seen in the regrowing PLM process after injury, including at the tip of the process and the growth cone (Figures S5G and S5H).

The GFP::CC domain fusion protein localized to puncta, similar to full-length PTRN-1::GFP (Figures 4C and S5), although the puncta were smaller and fewer in number. The GFP::CKK fusion protein was mostly diffuse, yet faint filaments could be seen in some axons close to the soma (Figure 4C). This localization differs from full-length PTRN-1::GFP, which strongly localizes to MT bundles if overexpressed (Figure S5E). The filamentous appearance of GFP::CKK suggests that any requirement for punctate localization of PTRN-1 can be bypassed if the CKK domain is expressed at high levels.

PTRN-1 Overexpression Can Promote Axon Branching in the Absence of DLK-1

DLK kinases are conserved regulators of axon regeneration in multiple organisms (Tedeschi and Bradke, 2013). In *C. elegans,* DLK-1 is essential for PLM and motor neuron axon regeneration (Hammarlund et al., 2009; Yan et al., 2009). DLK-1 acts via multiple targets, including the bZip transcription factor CEBP-1 (Yan et al., 2009) and the MT cytoskeleton (Chen et al., 2011; Ghosh-Roy et al., 2012). The *ptrn-1*(*0*) developmental defects in touch neurons partially resemble those caused by increased DLK-1 activity, suggesting that PTRN-1 may antagonize the DLK-1 pathway (Marcette et al., 2014; Richardson et al., 2014). We tested whether the DLK-1 pathway interacted with PTRN-1 in axon regeneration. *dlk-1*-null mutants are strongly blocked in PLM regrowth and lack regenerative growth cones (Figures 5A and 5B). *dlk-1*(*0*) *ptrn-1*(*0*) mutants displayed slightly more-severe defects in regrowth compared to *dlk-1*(*0*) (Figure 5A). Similarly, *cebp-1*(*0*) *ptrn-1*(*0*) showed further reduced regrowth compared to single mutants. These data suggest PTRN-1 does not antagonize the DLK-1 pathway in regeneration.

To further address the relationship of PTRN-1 and DLK-1, we overexpressed PTRN-1 in *dlk-1*(*0*) *ptrn-1*(*0*) double mutants. Overexpression of PTRN-1 did not suppress the regeneration defect in *dlk-1*(*0*), nor did it enhance regrowth from the severed axon stump. However, after injury, PTRN-1-overexpressing axons frequently extended one or more short collateral branches (Figures 5B and 5C); these were rarely seen in *dlk-1*(*0*) or in *dlk-1*(*0*) *ptrn-1*(*0*) animals after axotomy. Overexpression of the PTRN-1 CKK domain was also sufficient to induce formation of collateral branches after axon injury (Figures 5A and 5B). Strikingly, these collateral branches always grew posteriorly toward the PLM soma (Figure 5B). This effect of PTRN-1 overexpression was not observed in wild-type or in *ptrn-1*(*0*) single-mutant backgrounds (Figure 5C), suggesting it is dependent on loss of function in the DLK-1 pathway. Consistently, overexpression of PTRN-1 in the *cebp-1*(*0*) *ptrn-1*(*0*) mutant was also sufficient to trigger posteriorly directed branching after axotomy (Figures 5A–5C). The ability of PTRN-1 overexpression to induce neurite outgrowth in animals lacking DLK-1 pathway activity suggests that PTRN-1 can act either downstream or in parallel to the DLK-1 pathway.

The posterior orientation of PTRN-1-induced collateral branches suggested that axonal MT organization or polarity might be disrupted in these animals. However, the fraction of retrograde EBP comets in PLM axons was not significantly altered, indicating axonal MT polarity was normal (Figure S3). Notably, the increased numbers of dynamic MTs of *ptrn-1*(*0*) animals were fully suppressed in *ptrn-1*(*0*) *dlk-1*(*0*) double mutants (Figures 5D and 5E). DLK-1 overexpression can upregulate axonal MT dynamics in the absence of injury (Ghosh-Roy et al., 2012), correlating with increased axon regrowth (Hammarlund et al., 2009; Yan et al., 2009). Despite displaying upregulated dynamic MTs, *ptrn-1*(*0*) axons are unable to regrow efficiently, suggesting that PTRN-1 has additional functions important in regeneration.

DISCUSSION

We have shown that PTRN-1 is required for efficient axon regeneration in *C. elegans*. The role of PTRN-1 in regeneration is distinct from its function in development, in that PTRN-1 inhibits axon outgrowth (Marcette et al., 2014). Our observations of elevated MT dynamics in *ptrn-1* mutant axons provide insights into PTRN-1 function and identify Patronin/CAMSAPs as key players in axonal MT organization in regrowth.

PTRN-1 Protection from Kinesin-13/KLP-7 Is Required for Axonal Regrowth

Our results indicate that PTRN-1-dependent MT stabilization is required for normal regeneration. Loss of the MT depolymerase KLP-7 completely suppresses the axon regrowth defects of *ptrn-1*(*0*), suggesting excess destabilizing activity of KLP-7 impairs regrowth and that a low level of dynamic MTs is sufficient

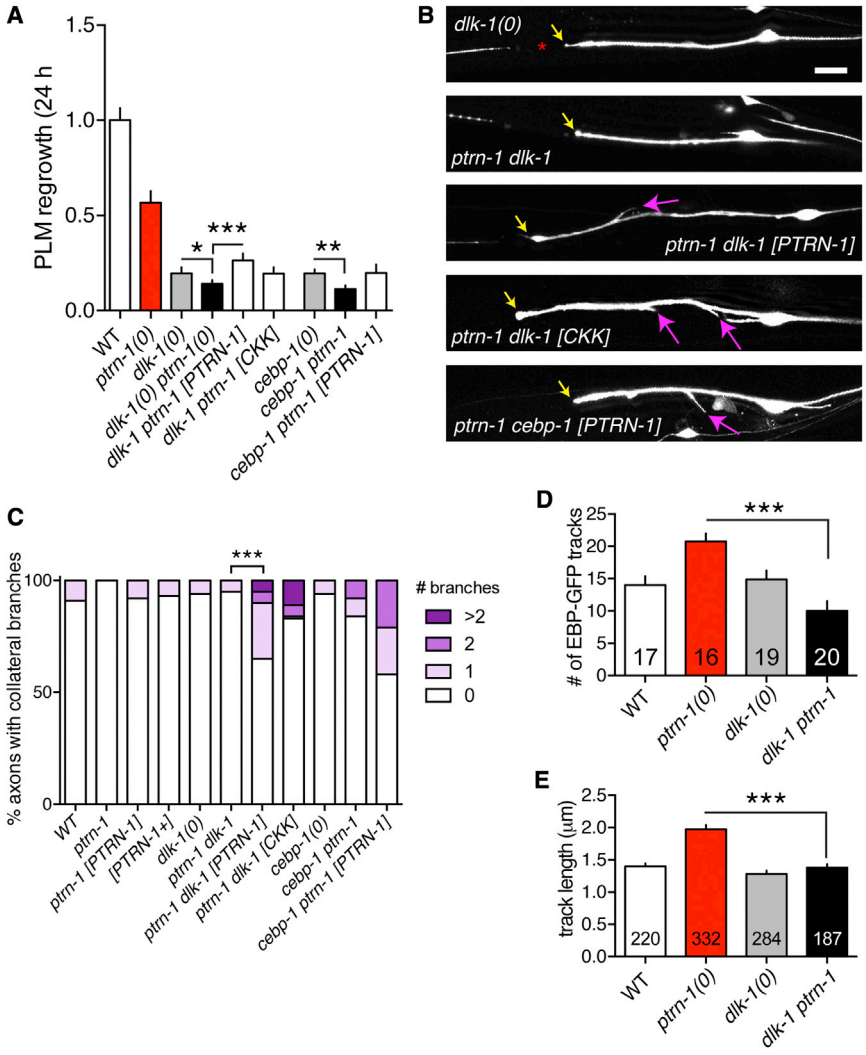

Figure 5. PTRN-1 Can Function Independently of DLK-1 in Regrowth and Collateral Branching after Injury

(A) PLM axon regeneration is severely impaired in *dlk-1*(*tm4024*) or *cebp-1*(*tm2807*) mutants; these defects are slightly enhanced in double mutants with *ptrn-1*(*0*). PTRN-1 overexpression causes increased growth in the *dlk-1*(*0*) *ptrn-1*(*0*) background due to increased collateral branching. Bars indicate mean ± SEM. Statistics: Mann-Whitney or t test. *$p < 0.05$.

(B) Collateral branches formed in PTRN-1 or CKK-overexpressing animals in *dlk-1* or *cebp-1* backgrounds (magenta arrowheads) are oriented toward the posterior. Representative confocal images of PLM 24 hpa; yellow arrows, axon stumps; scale: 10 μm.

(C) Overexpression of PTRN-1 in *dlk-1* pathway background leads to collateral branch formation after axotomy. Chi squared test; $n > 10$ animals per genotype.

(D and E) The elevated EBP::GFP comet number and track length of *ptrn-1*(*lt1*) mutants in the steady state is suppressed to wild-type levels in *dlk-1*(*0*) double mutants. Bars indicate mean ± SEM. Statistics: ANOVA; ***$p < 0.01$.

for regrowth. Expression of the PTRN-1 CKK domain was necessary and sufficient for its function in axon regeneration and restored MT dynamics to normal levels, indicating that the CKK domain alone can stabilize axonal MTs in vivo. Suppression of *ptrn-1*(*0*) phenotypes by loss of function in *klp-7* or by CKK overexpression also implies that MT stabilization can be sufficient for normal axon regrowth and therefore that the primary defect in *ptrn-1*(*0*) is in stabilization as opposed to minus-end anchoring. The CKK domain was sufficient to rescue *ptrn-1* defects but did not show a punctate distribution and instead weakly localized along filaments, presumably MT bundles. In contrast, the coiled-coil domain displayed punctate localization. These observations suggest that the minus-end-targeting mechanism of *C. elegans* PTRN-1 resembles that of *Drosophila* Patronin (Hendershott and Vale, 2014).

ptrn-1 Mutants Display Elevated Levels of Dynamic Axonal MTs

ptrn-1 mutants display consistently increased numbers of dynamic MTs in axons. This was unexpected, both in view of recent studies of CAMSAPs (see below) and because an increase in dynamic MTs correlates with enhanced regrowth in mutants such as *efa-6* (Chen et al., 2011). These observations suggest the absolute level of dynamic MTs may not be the critical determinant of regrowth capacity and that, instead, the change in the number of dynamic MTs after injury may be key. Alternatively, the ratio of dynamic to stable MTs may be important. Ultrastructural analysis confirms that *ptrn-1* mutants display fewer axonal MTs in the steady state (Richardson et al., 2014; this study). In either case, the increased number of dynamic MTs in *ptrn-1* appears to reflect MT destabilization, just as the reduced number of dynamic MTs in *klp-7* is due to hyperstabilization.

Our observations of increased numbers of dynamic MTs in *ptrn-1*(*0*) axons may be compared to a previous report that *ptrn-1*(*0*) mutants displayed fewer dynamic MTs in the dendrites of PHC sensory neurons (Richardson et al., 2014). This difference might reflect the opposing polarities of axonal MTs (oriented plus end out) versus dendritic MTs (in PHC, oriented with minus ends out) or differences in levels of free tubulin as the result of MT disruption in these different compartments. Dendritic MTs may be particularly dependent on PTRN-1. Indeed, knockdown of CAMSAP2 in mouse embryonic hippocampal neurons reduces the numbers of EBP comets most strongly in dendrites (Yau et al., 2014). Conversely, the upregulation of dynamic axonal MTs in *ptrn-1*(*0*) mutants could be a chronic response to the destabilization of the MT array in mature axons.

Relationship of PTRN-1 and DLK-1 in MT Dynamics and Regeneration

Consistent with the idea that increased dynamic MTs are a regulated response to MT destabilization, loss of function in *dlk-1* suppressed the upregulated MT dynamics of *ptrn-1*. However, *ptrn-1 dlk-1* double mutants display essentially normal numbers of dynamic axonal MTs. Thus, DLK-1-dependent MT upregulation does not mask an underlying loss of dynamic MTs. It is striking that, although PTRN-1 has opposite effects on dendritic and axonal MT dynamics (Richardson et al., 2014; this study), in both cases, loss of DLK-1 restores the number of dynamic MTs to normal levels. DLK-1 can sense MT depolymerization (Bounoutas et al., 2011) and may act homeostatically to upregulate or downregulate MT dynamics.

Our analysis of MT dynamics is consistent with the model that DLK-1 activity is upregulated in uninjured axons of *ptrn-1* mutants. However, PTRN-1 does not appear to inhibit DLK-1 in regeneration. *ptrn-1*(*0*) and *dlk-1*(*0*) mutants both displayed reduced regrowth and double mutants were further impaired, consistent with PTRN-1 and DLK-1 acting in concert. Overexpression of PTRN-1 was not sufficient to enhance axon regrowth in wild-type or in *dlk-1*(*0*). However, in the absence of DLK-1 pathway activity, the combination of axon injury and PTRN-1 overexpression induced collateral branching, suggesting PTRN-1 has a neurite-outgrowth-promoting activity that is normally repressed by the dominant DLK-1 pathway.

In conclusion, we have shown that PTRN-1 is critical for axon regrowth and that this role differs significantly from its function in development. Numerous questions remain to be addressed regarding PTRN-1's role in axon regeneration, and it will be of interest to examine the roles of CAMSAPs in other models of axon regeneration.

EXPERIMENTAL PROCEDURES

C. elegans Genetics

C. elegans strains were maintained on nematode growth medium agar plates between 15°C and 25°C using standard methods. We used the following published alleles and transgenes: *dlk-1*(*tm4024*); *klp-7*(*tm2143*); *cebp-1*(*tm2807*); P*mec-7*-GFP(*muls32*) for touch neurons, and P*unc-25*-GFP(*juls76*) for GABAergic motor neurons. *ptrn-1*(*ju698*) was isolated as a suppressor of an epidermal morphology mutant (A. Tong, M.C., and A.D.C., unpublished data) and creates a premature stop in PTRN-1A. *ptrn-1*(*tm5597*) was obtained from the Mitani lab. *ptrn-1*(*lt1*) was generated by MosDEL (Frøkjaer-Jensen et al., 2010) and deletes most of *ptrn-1* (S.W. and K.O., unpublished data). Plasmids were constructed by standard methods; new strains, plasmids, and transgenes are listed in Table S2.

Laser Axotomy, Confocal Imaging, and Image Analysis

Axon injury and regrowth imaging were performed as described (Wu et al., 2007). To image EBP-2::GFP dynamics, we used spinning-disk confocal microscopy essentially as described (Ghosh-Roy et al., 2012), using beads or 4 mM levamisole to immobilize animals. Movies were taken for 100–200 frames. For analysis of EBP::GFP dynamics in the ventral processes of GABAergic motor neurons, we analyzed a region of interest extending 30 μm anteriorly from the VD11 cell body (Figure S2B).

Statistics

Statistical analysis used GraphPad Prism. Categorical data were analyzed using the Chi squared or Fisher exact test. Continuous variables were tested for normality using the D'Agostino Pearson test; pairwise comparisons used Student's t test or the Mann-Whitney test; and multiple comparisons used one-way ANOVA or a Kruskal-Wallis test followed by a posttest.

SUPPLEMENTAL INFORMATION

Supplemental Information includes Supplemental Experimental Procedures, five figures, and two tables and can be found with this article online at http://dx.doi.org/10.1016/j.celrep.2014.09.054.

ACKNOWLEDGMENTS

ptrn-1(*ju698*) was isolated by Amy Tong and mapped by Tiffany Hsiao. We thank Zilu Wu for assistance with the femtosecond laser, Naina Kurup for P*unc-25*-EBP-2::GFP, the Japanese National Bioresource Project for *ptrn-1*(*tm5597*), and our lab members for advice and discussion. M.C. was supported by the UCSD Cellular and Molecular Genetics Training Grant (NIH T32 GM007240). K.O. receives salary and support from the Ludwig Institute for Cancer Research. Y.J. is an investigator and A.G. an associate of the Howard Hughes Medical Institute. This work was supported by R01 GM074207 to K.O. and NIH R01 NS057317 and GM054657 to A.D.C.

Received: August 10, 2014
Revised: September 15, 2014
Accepted: September 29, 2014
Published: October 23, 2014

REFERENCES

Baines, A.J., Bignone, P.A., King, M.D., Maggs, A.M., Bennett, P.M., Pinder, J.C., and Phillips, G.W. (2009). The CKK domain (DUF1781) binds microtubules and defines the CAMSAP/ssp4 family of animal proteins. Mol. Biol. Evol. *26*, 2005–2014.

Bounoutas, A., Kratz, J., Emtage, L., Ma, C., Nguyen, K.C., and Chalfie, M. (2011). Microtubule depolymerization in *Caenorhabditis elegans* touch receptor neurons reduces gene expression through a p38 MAPK pathway. Proc. Natl. Acad. Sci. USA *108*, 3982–3987.

Bradke, F., Fawcett, J.W., and Spira, M.E. (2012). Assembly of a new growth cone after axotomy: the precursor to axon regeneration. Nat. Rev. Neurosci. *13*, 183–193.

Chalfie, M., and Thomson, J.N. (1979). Organization of neuronal microtubules in the nematode *Caenorhabditis elegans*. J. Cell Biol. *82*, 278–289.

Chen, L., Wang, Z., Ghosh-Roy, A., Hubert, T., Yan, D., O'Rourke, S., Bowerman, B., Wu, Z., Jin, Y., and Chisholm, A.D. (2011). Axon regeneration pathways identified by systematic genetic screening in *C. elegans*. Neuron *71*, 1043–1057.

Chisholm, A.D. (2013). Cytoskeletal dynamics in *Caenorhabditis elegans* axon regeneration. Annu. Rev. Cell Dev. Biol. *29*, 271–297.

Conde, C., and Cáceres, A. (2009). Microtubule assembly, organization and dynamics in axons and dendrites. Nat. Rev. Neurosci. *10*, 319–332.

Ertürk, A., Hellal, F., Enes, J., and Bradke, F. (2007). Disorganized microtubules underlie the formation of retraction bulbs and the failure of axonal regeneration. J. Neurosci. *27*, 9169–9180.

Frøkjaer-Jensen, C., Davis, M.W., Hollopeter, G., Taylor, J., Harris, T.W., Nix, P., Lofgren, R., Prestgard-Duke, M., Bastiani, M., Moerman, D.G., and Jorgensen, E.M. (2010). Targeted gene deletions in *C. elegans* using transposon excision. Nat. Methods *7*, 451–453.

Ghosh-Roy, A., Goncharov, A., Jin, Y., and Chisholm, A.D. (2012). Kinesin-13 and tubulin posttranslational modifications regulate microtubule growth in axon regeneration. Dev. Cell *23*, 716–728.

Goodwin, S.S., and Vale, R.D. (2010). Patronin regulates the microtubule network by protecting microtubule minus ends. Cell *143*, 263–274.

Hammarlund, M., and Jin, Y. (2014). Axon regeneration in C. elegans. Curr. Opin. Neurobiol. *27*, 199–207.

Hammarlund, M., Nix, P., Hauth, L., Jorgensen, E.M., and Bastiani, M. (2009). Axon regeneration requires a conserved MAP kinase pathway. Science *323*, 802–806.

Hellal, F., Hurtado, A., Ruschel, J., Flynn, K.C., Laskowski, C.J., Umlauf, M., Kapitein, L.C., Strikis, D., Lemmon, V., Bixby, J., et al. (2011). Microtubule stabilization reduces scarring and causes axon regeneration after spinal cord injury. Science *331*, 928–931.

Hendershott, M.C., and Vale, R.D. (2014). Regulation of microtubule minus-end dynamics by CAMSAPs and Patronin. Proc. Natl. Acad. Sci. USA *111*, 5860–5865.

Jiang, K., Hua, S., Mohan, R., Grigoriev, I., Yau, K.W., Liu, Q., Katrukha, E.A., Altelaar, A.F., Heck, A.J., Hoogenraad, C.C., and Akhmanova, A. (2014). Microtubule minus-end stabilization by polymerization-driven CAMSAP deposition. Dev. Cell *28*, 295–309.

Keating, T.J., and Borisy, G.G. (1999). Centrosomal and non-centrosomal microtubules. Biol. Cell *91*, 321–329.

Kirszenblat, L., Neumann, B., Coakley, S., and Hilliard, M.A. (2013). A dominant mutation in mec-7/β-tubulin affects axon development and regeneration in Caenorhabditis elegans neurons. Mol. Biol. Cell *24*, 285–296.

Lin, J.Y., Sann, S.B., Zhou, K., Nabavi, S., Proulx, C.D., Malinow, R., Jin, Y., and Tsien, R.Y. (2013). Optogenetic inhibition of synaptic release with chromophore-assisted light inactivation (CALI). Neuron *79*, 241–253.

Liu, K., Tedeschi, A., Park, K.K., and He, Z. (2011). Neuronal intrinsic mechanisms of axon regeneration. Annu. Rev. Neurosci. *34*, 131–152.

Marcette, J.D., Chen, J.J., and Nonet, M.L. (2014). The *Caenorhabditis elegans* microtubule minus-end binding homolog PTRN-1 stabilizes synapses and neurites. eLife *3*, e01637.

Meng, W., Mushika, Y., Ichii, T., and Takeichi, M. (2008). Anchorage of microtubule minus ends to adherens junctions regulates epithelial cell-cell contacts. Cell *135*, 948–959.

Moore, D.L., Blackmore, M.G., Hu, Y., Kaestner, K.H., Bixby, J.L., Lemmon, V.P., and Goldberg, J.L. (2009). KLF family members regulate intrinsic axon regeneration ability. Science *326*, 298–301.

Nguyen, M.M., Stone, M.C., and Rolls, M.M. (2011). Microtubules are organized independently of the centrosome in Drosophila neurons. Neural Dev. *6*, 38.

Nguyen, M.M., McCracken, C.J., Milner, E.S., Goetschius, D.J., Weiner, A.T., Long, M.K., Michael, N.L., Munro, S., and Rolls, M.M. (2014). Γ-tubulin controls neuronal microtubule polarity independently of Golgi outposts. Mol. Biol. Cell *25*, 2039–2050.

Ori-McKenney, K.M., Jan, L.Y., and Jan, Y.N. (2012). Golgi outposts shape dendrite morphology by functioning as sites of acentrosomal microtubule nucleation in neurons. Neuron *76*, 921–930.

Park, K.K., Liu, K., Hu, Y., Smith, P.D., Wang, C., Cai, B., Xu, B., Connolly, L., Kramvis, I., Sahin, M., and He, Z. (2008). Promoting axon regeneration in the adult CNS by modulation of the PTEN/mTOR pathway. Science *322*, 963–966.

Richardson, C.E., Spilker, K.A., Cueva, J.G., Perrino, J., Goodman, M.B., and Shen, K. (2014). PTRN-1, a microtubule minus end-binding CAMSAP homolog, promotes microtubule function in *Caenorhabditis elegans* neurons. eLife *3*, e01498.

Sahly, I., Khoutorsky, A., Erez, H., Prager-Khoutorsky, M., and Spira, M.E. (2006). On-line confocal imaging of the events leading to structural dedifferentiation of an axonal segment into a growth cone after axotomy. J. Comp. Neurol. *494*, 705–720.

Sengottuvel, V., Leibinger, M., Pfreimer, M., Andreadaki, A., and Fischer, D. (2011). Taxol facilitates axon regeneration in the mature CNS. J. Neurosci. *31*, 2688–2699.

Shu, X., Lev-Ram, V., Deerinck, T.J., Qi, Y., Ramko, E.B., Davidson, M.W., Jin, Y., Ellisman, M.H., and Tsien, R.Y. (2011). A genetically encoded tag for correlated light and electron microscopy of intact cells, tissues, and organisms. PLoS Biol. *9*, e1001041.

Stepanova, T., Slemmer, J., Hoogenraad, C.C., Lansbergen, G., Dortland, B., De Zeeuw, C.I., Grosveld, F., van Cappellen, G., Akhmanova, A., and Galjart, N. (2003). Visualization of microtubule growth in cultured neurons via the use of EB3-GFP (end-binding protein 3-green fluorescent protein). J. Neurosci. *23*, 2655–2664.

Stiess, M., Maghelli, N., Kapitein, L.C., Gomis-Rüth, S., Wilsch-Bräuninger, M., Hoogenraad, C.C., Tolić-Nørrelykke, I.M., and Bradke, F. (2010). Axon extension occurs independently of centrosomal microtubule nucleation. Science *327*, 704–707.

Stone, M.C., Nguyen, M.M., Tao, J., Allender, D.L., and Rolls, M.M. (2010). Global up-regulation of microtubule dynamics and polarity reversal during regeneration of an axon from a dendrite. Mol. Biol. Cell *21*, 767–777.

Tedeschi, A., and Bradke, F. (2013). The DLK signalling pathway—a double-edged sword in neural development and regeneration. EMBO Rep. *14*, 605–614.

Topalidou, I., Keller, C., Kalebic, N., Nguyen, K.C., Somhegyi, H., Politi, K.A., Heppenstall, P., Hall, D.H., and Chalfie, M. (2012). Genetically separable functions of the MEC-17 tubulin acetyltransferase affect microtubule organization. Curr. Biol. *22*, 1057–1065.

Wang, H., Brust-Mascher, I., Civelekoglu-Scholey, G., and Scholey, J.M. (2013). Patronin mediates a switch from kinesin-13-dependent poleward flux to anaphase B spindle elongation. J. Cell Biol. *203*, 35–46.

Wu, Z., Ghosh-Roy, A., Yanik, M.F., Zhang, J.Z., Jin, Y., and Chisholm, A.D. (2007). *Caenorhabditis elegans* neuronal regeneration is influenced by life stage, ephrin signaling, and synaptic branching. Proc. Natl. Acad. Sci. USA *104*, 15132–15137.

Xiong, X., Wang, X., Ewanek, R., Bhat, P., Diantonio, A., and Collins, C.A. (2010). Protein turnover of the Wallenda/DLK kinase regulates a retrograde response to axonal injury. J. Cell Biol. *191*, 211–223.

Yan, D., and Jin, Y. (2012). Regulation of DLK-1 kinase activity by calcium-mediated dissociation from an inhibitory isoform. Neuron *76*, 534–548.

Yan, D., Wu, Z., Chisholm, A.D., and Jin, Y. (2009). The DLK-1 kinase promotes mRNA stability and local translation in C. elegans synapses and axon regeneration. Cell *138*, 1005–1018.

Yau, K.W., van Beuningen, S.F., Cunha-Ferreira, I., Cloin, B.M., van Battum, E.Y., Will, L., Schätzle, P., Tas, R.P., van Krugten, J., Katrukha, E.A., et al. (2014). Microtubule minus-end binding protein CAMSAP2 controls axon specification and dendrite development. Neuron *82*, 1058–1073.

Zhou, K., Stawicki, T.M., Goncharov, A., and Jin, Y. (2013). Position of UNC-13 in the active zone regulates synaptic vesicle release probability and release kinetics. eLife *2*, e01180.